Journal of Engineering Mathematics, Vol. 11, No. 4, October 1977
Noordhoff International Publishing–Leyden
Printed in The Netherlands

Numerical determination of the fundamental eigenvalue for the Laplace operator on a spherical domain

H. WALDEN

NASA/Goddard Space Flight Center, Greenbelt, Maryland, U.S.A.

R. B. KELLOGG

Institute for Fluid Dynamics and Applied Mathematics, University of Maryland, College Park, Maryland, U.S.A.

(Received June 1, 1976 and in revised form December 6, 1976)

SUMMARY

Methods for obtaining approximate solutions for the fundamental eigenvalue of the Laplace–Beltrami operator (i.e., the membrane eigenvalue problem for the vibration equation) on the unit spherical surface are developed. Two types of spherical surface domains are considered: (1) the interior of a spherical triangle, and (2) the exterior of a great circle arc extending for less than π radians (a spherical surface with a slit). In both cases, zero boundary conditions are imposed. In order to solve the resulting second-order elliptic partial differential equations in two independent variables, a finite difference approximation is employed. The fundamental eigenvalue is approximated by iteration utilizing the power method and point successive overrelaxation. Some numerical results are given and compared, in certain special cases, with analytical solutions to the eigenvalue problem. The significance of the numerical eigenvalue results is discussed in terms of the singularities in the solution of three-dimensional boundary-value problems near a polyhedral corner of the domain.

1. Introduction

Boundary-value problems for a partial differential equation which involves the Laplacian arise naturally in a wide variety of applications to physics and engineering, such as in determining the gravitational or electrostatic potential, in solving Maxwell's equations of electromagnetism, and in the theory of elasticity. When the region of the boundary-value problem contains corners or edges, the solution may become singular in the vicinity of such corners or edges. Furthermore, the nature of the singularity may play a fundamental role in the physical application.

In two-dimensional problems, the singularities in the solution near a corner of a domain have been studied thoroughly and are well understood [1, 2]. For instance, the well-known $r^{-\frac{1}{2}}$ singularity in the stresses is of significance in the theory of crack propagation in brittle materials and in the numerical solution of crack problems [3]. In contrast, relatively little is known about the solution of a three-dimensional boundary-value problem near an edge or corner of the domain [4, 5]. A preliminary discussion of singularities in three-dimensional elasticity problems appears in [6, 7]. A study of three-dimensional singularities relating to the distribution of electrostatic charge in a flat conducting plate is given in [8]. Further knowledge about the nature of three-dimensional singularities would be of importance to many areas of application.

Consider the solution $v(x, y, z)$ of the Dirichlet problem:

$$\Delta v = f \text{ in } G, \quad v = 0 \text{ on } \partial G, \tag{1}$$

where G is a polyhedron with boundary ∂G, v and f are defined in G, and $\Delta v = v_{xx} + v_{yy} + v_{zz}$ denotes the Laplacian of v. It is known [4] that the derivatives of v may become singular near a vertex of G, and the severity of the singularity is determined by the fundamental eigenvalue of an associated eigenvalue problem for the Laplace–Beltrami operator on the unit sphere. Methods for obtaining approximate solutions of this associated eigenvalue problem will be considered in this paper. Some results will be tabulated, and their implications for the singularity in v will be discussed.

If spherical co-ordinates are introduced such that $x = r \sin \phi \cos \theta$, $y = r \sin \phi \sin \theta$, and $z = r \cos \phi$, with $0 \leq \phi \leq \pi$ and $0 \leq \theta < 2\pi$, then the Laplacian may be written [9, p. 225]

$$\Delta u = r^{-2}(r^2 u_r)_r + r^{-2} \Lambda u, \tag{2}$$

where

$$\Lambda u = \csc \phi [(u_\theta \csc \phi)_\theta + (u_\phi \sin \phi)_\phi]. \tag{3}$$

If the origin of the co-ordinate system is placed at a vertex of G, then the singularity at the origin in the solution of problem (1) is related to the eigenvalue problem

$$\Lambda u + \lambda u = 0 \text{ in } D, \quad u = 0 \text{ on } \partial D, \tag{4}$$

where D represents the region on the surface of a small sphere (centered at the origin) bounded by the polyhedron G. In this paper, the case in which the region D is a spherical triangle T, will be considered first, to be followed by a discussion of the case in which D is a slit domain, consisting of the exterior of an arc of a great circle on the sphere.

Without loss of generality, it may be assumed that $r = 1$. The boundary ∂D will consist of arcs of three great circles on the unit sphere. The spherical co-ordinate system is defined so that the origin of co-ordinates is at the center of the sphere, the z-axis intersects the unit sphere at a vertex of T, and the x, z-plane contains a side of T which is less than π radians in length. The relevant arcs of the three great circles specifying T are then given by

$$\theta = 0, \quad \theta = \Theta, \quad z = ax + by, \tag{5a, b, c}$$

where Θ, a, and b are constants (see Figure 1). Equation (5c), in spherical co-ordinates, becomes

$$\cot \phi = a \cos \theta + b \sin \theta. \tag{6}$$

Equations (5a), (5b), and (6) define two domains on the sphere, the region $R(\Theta, a, b)$ specified by

$$0 < \theta < \Theta, \quad \cot \phi > a \cos \theta + b \sin \theta, \tag{7}$$

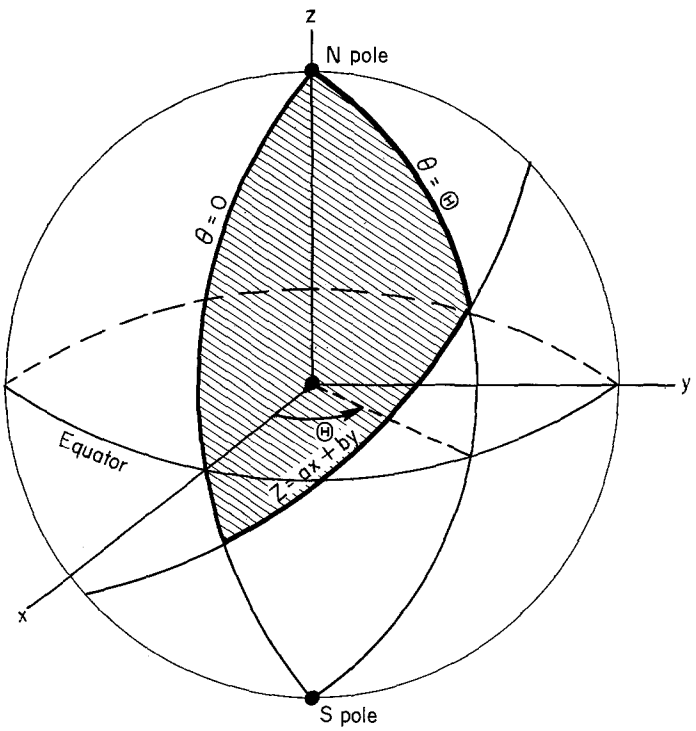

Figure 1. The spherical triangle T (its interior R is shown shaded) bounded by arcs of three great circles, specified by the parameters Θ, a, and b.

and the region $S(\Theta, a, b)$ complementary to R. Both the interior R and the exterior S of the spherical triangle T are thus determined by the parameters Θ, a, and b, which satisfy $0 \leq \Theta < 2\pi$, and $-\infty < a, b < \infty$. The eigenvalue problem (4) for the unit sphere,

$$u_{\theta\theta} \csc \phi + (u_\phi \sin \phi)_\phi + \lambda u \sin \phi = 0 \text{ in } D, \tag{8a}$$

$$u = 0 \text{ on } \partial D, \tag{8b}$$

where D represents either R or S, has a denumerably infinite sequence of positive eigenvalues which may be ordered [9, p. 298] so that $0 < \lambda_1 < \lambda_2 \leq \lambda_3 \leq \ldots$, as well as a corresponding sequence of linearly independent eigenfunctions $u_1, u_2, \ldots$. In this paper, the fundamental (smallest positive) eigenvalue of equation (8a) will be determined, subject to the boundary condition (8b), for the following two cases: (1) when D is the interior R of a spherical triangle, and (2) when D is the exterior S of a spherical "triangle" which has degenerated to a line in the special situation: $\Theta = 0$. In order to solve the second-order elliptic partial differential equation (8a) in two independent variables θ, ϕ, a finite difference approximation is derived. The resulting finite difference equations are written in matrix form and then solved by the iterative method of point successive overrelaxation. Upon convergence, the fundamental eigenvalue is found by iteration utilizing the power method as applied to the finite Rayleigh quotient. Numerical results for a number of cases are presented, and the implications for the singularities in three-dimensional polyhedral boundary-value problems are discussed.

2. Finite difference approximation

In problems involving elliptic partial differential equations for which a general analytic solution is not known, such as equation (8), the method of finite differences is commonly employed to determine numerical results. In the following, the domain D on the spherical surface is taken to be the interior $R(\Theta, a, b)$ of a spherical triangle, with $0 < \Theta < 2\pi$. A rectangular network of grid points (θ_i, ϕ_j), $i = 0, 1, 2, \ldots, N_\theta$; $j = 0, 1, 2, \ldots, N_\phi$ is established throughout the θ, ϕ-plane. N_θ and N_ϕ represent the number of grid intervals in the θ- and ϕ-directions, respectively, so that $h_\theta N_\theta = \Theta$, where h_θ is the constant grid spacing in the θ-direction. In consideration of the singularity at the north pole, where two boundaries of the spherical triangle meet at a point with a discontinuous tangent (i.e., a corner), variable grid spacing in the ϕ-direction is introduced through the parameter,

$$h_{\phi,j} = \phi_j - \phi_{j-1} > 0, \qquad j = 1, 2, \ldots, N_\phi. \tag{9}$$

Grid points in the ϕ-direction are specified by

$$\phi_j = \begin{cases} \left(\dfrac{2j}{N_\phi}\right)^\gamma \dfrac{\pi}{2} & \text{for } j = 0, 1, 2, \ldots, \tfrac{1}{2}N_\phi; \\ \pi - \phi_{N_\phi - j} & \text{for } j = \tfrac{1}{2}N_\phi + 1, \tfrac{1}{2}N_\phi + 2, \ldots, N_\phi, \end{cases} \tag{10}$$

where N_ϕ is assumed to be an even integer and γ is a positive constant. If $\gamma = 1$, then formula (10) reduces to a uniform grid spacing, $\phi_j = j\pi/N_\phi$, for all j, where N_ϕ need not be even. If $\gamma > 1$, the density of grid points increases toward the poles, $\phi_0 = 0$ and $\phi_{N_\phi} = \pi$, and decreases toward the equator, $\phi_{N_\phi/2} = \pi/2$, and conversely, if $\gamma < 1$. For all γ, grid points in the ϕ-direction are symmetrically placed about the center point or equator.

If the exact solution to equation (8a) is denoted $u = u(\theta, \phi)$, then let its approximation at each grid point be $U = U(\theta_i, \phi_j) = U_{i,j}$. To approximate the second-order partial derivative in the first term of equation (8a), the centered second difference quotient [10, pp. 430–431],

$$u_{\theta\theta} \cong \frac{1}{h_\theta^2}(U_{i+1,j} - 2U_{i,j} + U_{i-1,j}), \tag{11}$$

is utilized. Using the midway (or averaged) grid points,

$$\left.\begin{aligned} \phi_{j+\frac{1}{2}} &= \tfrac{1}{2}(\phi_j + \phi_{j+1}) \\ \phi_{j-\frac{1}{2}} &= \tfrac{1}{2}(\phi_j + \phi_{j-1}) \end{aligned}\right\} j = 1, 2, \ldots, N_\phi - 1, \tag{12}$$

the first-order partial derivative in the second term of equation (8a) may be approximated by a centered midway first difference quotient,

$$(u_\phi \sin\phi)_\phi \cong \frac{(u_\phi)_{i,j+\frac{1}{2}} \sin\phi_{j+\frac{1}{2}} - (u_\phi)_{i,j-\frac{1}{2}} \sin\phi_{j-\frac{1}{2}}}{\tfrac{1}{2}(h_{\phi,j+1} + h_{\phi,j})}. \tag{13}$$

To approximate the terms involving u_ϕ, a centered first difference quotient is employed:

$$(u_\phi)_{i,j+\frac{1}{2}} \cong \frac{U_{i,j+1} - U_{i,j}}{h_{\phi,j+1}}, \quad (u_\phi)_{i,j-\frac{1}{2}} \cong \frac{U_{i,j} - U_{i,j-1}}{h_{\phi,j}}. \tag{14}$$

Combining equations (13) and (14) results in the approximation,

$$(u_\phi \sin\phi)_\phi \cong \frac{2\sin\phi_{j+\frac{1}{2}}}{h_{\phi,j+1}+h_{\phi,j}}\cdot\frac{U_{i,j+1}-U_{i,j}}{h_{\phi,j+1}} - \frac{2\sin\phi_{j-\frac{1}{2}}}{h_{\phi,j+1}+h_{\phi,j}}\cdot\frac{U_{i,j}-U_{i,j-1}}{h_{\phi,j}}. \tag{15}$$

The finite difference approximation to equation (8a) may be written, by use of equations (11) and (15), as

$$(U_{i+1,j}-2U_{i,j}+U_{i-1,j})\frac{\csc\phi_j}{h_\theta^2} + \frac{2\sin\phi_{j+\frac{1}{2}}}{h_{\phi,j+1}+h_{\phi,j}}\left(\frac{U_{i,j+1}-U_{i,j}}{h_{\phi,j+1}}\right)$$
$$-\frac{2\sin\phi_{j-\frac{1}{2}}}{h_{\phi,j+1}+h_{\phi,j}}\left(\frac{U_{i,j}-U_{i,j-1}}{h_{\phi,j}}\right)+\lambda U_{i,j}\sin\phi_j = 0. \tag{16}$$

Appropriate multiplication and re-arrangement of terms yields a symmetric five-point difference equation of the form:

$$a_jU_{i,j} - b_jU_{i+1,j} - c_jU_{i,j+1} - b_jU_{i-1,j} - c_{j-1}U_{i,j-1} = \lambda e_jU_{i,j}, \tag{17}$$

where

$$b_j = \frac{\csc\phi_j}{h_\theta^2}(h_{\phi,j+1}+h_{\phi,j}), \tag{18a}$$

$$c_j = \frac{2\sin\phi_{j+\frac{1}{2}}}{h_{\phi,j+1}}, \tag{18b}$$

$$e_j = (h_{\phi,j+1}+h_{\phi,j})\sin\phi_j, \tag{18c}$$

and

$$a_j = 2b_j + c_j + c_{j-1}. \tag{18d}$$

In terms of grid points in the ϕ-direction, by virtue of equations (9) and (12),

$$b_j = \frac{\phi_{j+1}-\phi_{j-1}}{h_\theta^2\sin\phi_j} > 0, \tag{19a}$$

$$c_j = \frac{2\sin\frac{1}{2}(\phi_j+\phi_{j+1})}{\phi_{j+1}-\phi_j} > 0, \tag{19b}$$

and

$$e_j = (\phi_{j+1}-\phi_{j-1})\sin\phi_j > 0. \tag{19c}$$

The boundary conditions (8b) must be imposed on the discretized version (17) of the eigenvalue equation. Along the meridional boundaries (5a) and (5b), $U_{0,j} = U_{N_\theta,j} = 0$ for

all j, and $U_{i,j} = 0$ for those grid points (i, j) such that

$$\cot \phi_j \leq a \cos \theta_i + b \sin \theta_i, \tag{20}$$

as a result of condition (7) pertaining to the spherical triangle interior R. Furthermore, $U_{i,0} = U_{i,N_\phi} = 0$ for all i, at the north and south poles of the sphere. In the limiting cases of $a, b \to -\infty$ (either or both), the triangle boundary, according to equation (6), includes the south pole, $\phi = \pi$.

3. Iterative calculation of the fundamental eigenvalue

In a matrix formulation of the finite difference equation (17), let I denote the number of grid points which are interior to the spherical triangle, i.e., those which violate inequality (20). Let U represent an I-dimensional vector whose components are the unknown values $U_{i,j}$ associated with the interior grid points. The components of U are ordered rowwise, such that successive constant ϕ grid lines are each scanned in order of increasing θ values. With this natural ordering of the grid points [11, p. 187], equation (17) may be written in matrix form as $AU = \lambda EU$, where A and E are symmetric square matrices of order I. A is sparse and consists of positive diagonal entries and non-positive off-diagonal entries, while E is a diagonal matrix with positive diagonal entries. The entries of both A and E depend only on the j index. Define a square matrix V of order I by $V = E^{\frac{1}{2}}U$, where $E^{\frac{1}{2}}$ is the diagonal matrix consisting of entries which are equal, respectively, to the square roots of the elements of E. With this definition, the matrix form of equation (17) may be transformed to

$$\tilde{A}V = E^{-\frac{1}{2}}AE^{-\frac{1}{2}}V = \lambda V, \tag{21}$$

where the diagonal matrix $E^{-\frac{1}{2}}$ is the inverse of $E^{\frac{1}{2}}$ formed by taking reciprocals of the respective diagonal entries of $E^{\frac{1}{2}}$. The matrix $\tilde{A} \equiv E^{-\frac{1}{2}}AE^{-\frac{1}{2}}$ retains the symmetry property.

The fundamental eigenvalue of $\tilde{A}$ may be determined by the power method [12, pp. 147ff; 13, pp. 355–356]. Define the sequence of vectors,

$$V^{(m+1)} = \lambda^{(m)}\tilde{A}^{-1}V^{(m)}, \qquad m = 1, 2, \ldots, \tag{22}$$

where the scalars $\lambda^{(m)}$ are given by the ratios of inner products,

$$\lambda^{(m)} = \frac{(V^{(m)}, V^{(m)})}{(\tilde{A}^{-1}V^{(m)}, V^{(m)})}, \qquad m = 1, 2, \ldots. \tag{23}$$

The limit $V^{(m)}$ as $m \to \infty$ is the eigenvector associated with the fundamental eigenvalue of $\tilde{A}$, the latter of which is approximated by the finite Rayleigh quotient (23). In terms of the original vector U, it is seen that $U^{(m)} = E^{-\frac{1}{2}}V^{(m)}$ and $\tilde{A}^{-1} = E^{\frac{1}{2}}A^{-1}E^{\frac{1}{2}}$, so that equations (22) and (23) become

$$U^{(m+1)} = \lambda^{(m)}A^{-1}EU^{(m)}, \qquad m = 1, 2, \ldots \tag{24}$$

and

$$\lambda^{(m)} = \frac{(U^{(m)}, EU^{(m)})}{(A^{-1}EU^{(m)}, EU^{(m)})}, \qquad m = 1, 2, \ldots \tag{25}$$

As an initial estimate, $U^{(1)}$ is defined to have all components equal to unity.

The power method (24)–(25) requires solving equations of the general form $AU = F$ for the vector U, where F represents the vector iterates $EU^{(m)}$. For this purpose, the iterative method of point successive overrelaxation [11, pp. 58–59] is applied to the system of linear equations (17) and produces iterates $U^{(k)}$ whose components are given by

$$U_{i,j}^{(k+1)} = \frac{\omega}{a_j}[b_j U_{i+1,j}^{(k)} + c_j U_{i,j+1}^{(k)} + b_j U_{i-1,j}^{(k+1)} + c_{j-1} U_{i,j-1}^{(k+1)} + F_{i,j}] + (1-\omega)U_{i,j}^{(k)},$$
$$k = 1, 2, \ldots \quad (26)$$

The k-superscripts indicate an iteration process, here called the inner iterations, distinct from the m-iterates, or outer iterations, specified in the power method. The vectors U and F, of course, depend upon the iteration index m, although this has not been indicated explicitly in equation (26), so as to preserve legibility. The vector inner products in the Rayleigh quotient (25) may be written in component form as

$$(U^{(m)}, EU^{(m)}) = \sum_i \left(\sum_j \frac{F_{i,j}^2}{e_j} \right) \quad (27a)$$

and

$$(A^{-1}EU^{(m)}, EU^{(m)}) = \sum_i \left(\sum_j F_{i,j} U_{i,j} \right), \quad (27b)$$

where the double summations are taken over grid points interior to the spherical triangle. The scalar relaxation factor ω is evaluated, as described below, based upon the maximum component norms for successive inner iterates of the vector U,

$$\varepsilon^{(k)} \equiv \max_{i,j} |U_{i,j}^{(k+1)} - U_{i,j}^{(k)}|, \qquad k = 1, 2, \ldots \quad (28a)$$

and the ratios,

$$r^{(k)} \equiv \varepsilon^{(k)}/\varepsilon^{(k-1)}, \qquad k = 2, 3, \ldots, \quad (28b)$$

calculated during the inner iterations.

Convergence of the successive overrelaxation (S.O.R.) iterates (26) for any initial vector $U^{(1)}$ and for a relaxation factor in the range $0 < \omega < 2$ follows from the Ostrowski–Reich theorem [14, p. 123] and the fact that A may be shown to be a symmetric irreducibly diagonally dominant matrix with positive diagonal entries, which is therefore positive definite [11, p. 23]. Although the S.O.R. method will converge for all ω such that $0 < \omega < 2$, the most rapid convergence occurs for an optimal value ω_{opt}, where $1 < \omega_{\text{opt}} < 2$. A theoretical expression for ω_{opt} exists [11, p. 110] since the Jacobi matrix B associated with the matrix A is cyclic of index 2, but this expression depends on the spectral radius of B, a quantity that is not, unfortunately, known *a priori*. To overcome this difficulty in determining ω_{opt}, a numerical technique [13, pp. 369–370] is applied. If ω is set equal to unity in equation (26), then the S.O.R. method reduces to the point Gauss–Seidel iterative

method, in which case the parameters defined in equations (28) will converge to a value,

$$\lim_{k\to\infty} r^{(k)} = r \leq 1, \tag{29}$$

equal to the square of the desired spectral radius of B. Then ω_{opt} can be computed by

$$\omega_{\text{opt}} = \frac{2}{1+\sqrt{1-r}}. \tag{30}$$

The algorithm utilized for the solution of the eigenvalue problem on a digital computer, described in detail in [15], is a modification of a method suggested in [13, pp. 375–376].

4. Analytic solutions for special cases

The elliptic partial differential equation (8a) can be solved analytically for certain special cases, and such exact solutions are useful in providing checks upon numerical calculations based upon the finite difference approximation. Using the separation of variables technique, in which $u(\theta, \phi) = X(\theta)Y(\phi)$, the analytic solution to equation (8a) is known [9, pp. 314ff, 510ff] to consist of the Laplace spherical harmonics,

$$X(\theta) = A \sin k\theta + B \cos k\theta, \tag{31a}$$

$$Y(\phi) = P_{n,k}(\cos\phi) = (1-z^2)^{k/2}\frac{\mathrm{d}^k}{\mathrm{d}z^k}P_n(z), \qquad k = 0, 1, 2, \ldots, n, \tag{31b}$$

where A and B are arbitrary constants, k^2 is a separation constant, n is defined by $\lambda = n(n+1)$, and $P_{n,k}$ are the associated Legendre functions of order k. The Legendre functions of order zero, $P_n(z) = P_{n,0}(z)$, are polynomials in $z \equiv \cos\phi$ of degree n. The boundary condition (8b) requires that $u(0, \phi) = u(\Theta, \phi) = 0$, so that the solution (31a) becomes

$$X(\theta) = A \sin\left(\frac{\pi}{\Theta}\right)\theta, \tag{32}$$

where $k = \pi/\Theta$ is chosen so that $X(\theta)$ vanishes only at the endpoints of the interval, $0 \leq \theta \leq \Theta$.

For the special case $k = n$, $Y(\phi)$ reduces to a multiple of $(\sin\phi)^k$ and the solution $X(\theta)Y(\phi)$ is

$$u(\theta, \phi) = A \sin\left(\frac{\pi\theta}{\Theta}\right)(\sin\phi)^{\pi/\Theta}, \tag{33}$$

with the corresponding eigenvalue,

$$\lambda = \frac{\pi}{\Theta}\left(\frac{\pi}{\Theta}+1\right). \tag{34}$$

When $A \neq 0$, the eigenfunction (33) vanishes only for $\theta = 0, \Theta$ and $\phi = 0, \pi$ in the domain, $0 \leq \theta \leq \Theta < 2\pi; 0 \leq \phi \leq \pi$, and thus represents a solution for a two-sided spherical wedge-shaped domain bounded by meridional great circle arcs extending between the north and south poles. The wedge domain is the degenerate spherical triangle $R(\Theta, 0, -\infty)$ when $0 < \Theta \leq \pi$; however, when $\pi < \Theta < 2\pi$, the wedge does not appear as a limiting case of the spherical triangle.

For the special case $k = n - 1$, since the Legendre functions $P_n(z)$ are polynomials in z containing terms only of even or odd powers of z, as n is even or odd, respectively, then $Y(\phi)$ reduces to a multiple of $(\sin \phi)^k \cos \phi$, and the solution $X(\theta)Y(\phi)$ is

$$u(\theta, \phi) = A \sin\left(\frac{\pi\theta}{\Theta}\right)(\sin \phi)^{\pi/\Theta} \cos \phi, \tag{35}$$

with the corresponding eigenvalue,

$$\lambda = \left(\frac{\pi}{\Theta} + 1\right)\left(\frac{\pi}{\Theta} + 2\right). \tag{36}$$

For $A \neq 0$, the eigenfunction (35) has the same zeroes as previously with an additional zero at $\phi = \pi/2$. Thus, equation (35) represents an exact solution for the spherical triangle defined by the domain, $0 \leq \theta \leq \Theta < 2\pi; 0 \leq \phi \leq \pi/2$, which is bounded by two meridional arcs and the equator, viz., $R(\Theta, 0, 0)$ for $0 < \Theta < 2\pi$.

In the limit $\Theta = 2\pi$, the solution (33) is $u(\theta, \phi) = A \sin(\theta/2)(\sin \phi)^{\frac{1}{2}}$, with corresponding eigenvalue $\lambda = \frac{3}{4}$. The wedge domain becomes the entire surface of the sphere except for a boundary great circle arc $\theta = 0, 0 \leq \phi \leq \pi$ extending between the poles. Equivalently, this domain is the exterior of a spherical triangle in the limit $\Theta = 0$, as will become significant in the problem of a slit spherical surface discussed later. In the limit $\Theta = 2\pi$, the solution (35) is $u(\theta, \phi) = A \sin(\theta/2)(\sin \phi)^{\frac{1}{2}} \cos \phi$, with corresponding $\lambda = \frac{15}{4}$. The degenerate spherical triangle domain $R(2\pi, 0, 0)$ is the entire upper hemisphere excluding a boundary great circle arc $\theta = 0, 0 \leq \phi \leq \pi/2$ extending from the north pole to the equator.

5. Discussion of numerical results

Consider first spherical triangles which contain two right angles and where the boundary great circle arcs are formed by the equator, $z = 0$, and two meridional arcs. Such spherical triangles $R(\Theta, 0, 0)$, where $0 < \Theta < 2\pi$, are associated with the fundamental eigenvalue (36). Table 1 displays calculated and exact values for λ for three values of Θ and for various rectangular grids, all of which utilize constant θ- and ϕ-spacing ($\gamma = 1$). For all numerical results discussed in this paper, convergence criteria of 10^{-6} are used for terminating both the inner iterations, through the maximum component norm (28a), and the outer iterations, through absolute differences of successive values of the Rayleigh quotient (25). Table 1 includes the calculated value for the optimal ω, the required number m of outer iterations to achieve convergence in λ, and the required number k_m of inner iterations to achieve convergence of U by S.O.R. for the final outer iteration. The relative error in λ, given by $(\lambda_{\text{exact}} - \lambda_{\text{calculated}})/\lambda_{\text{exact}}$, is approximately 0.03 for the $N_\theta = N_\phi = 10$ grids, and 0.008, 0.003,

TABLE 1

Fundamental eigenvalues of double right spherical triangles ($a = b = 0$) using constant grid spacing ($\gamma = 1$)

Spherical triangle parameter Θ	*Rectangular grid parameters* $N_\theta = N_\phi$	*Fundamental eigenvalue* λ		*Optimal scalar relaxation factor* ω	*Required number of outer iterations* m	*Required number of S.O.R. inner iterations at convergence* k_m
		Calculated value	*Exact value*			
π	10	5.831	6	1.460	8	24
π	20	5.958	6	1.695	8	48
π	30	5.981	6	1.796	8	71
π	40	5.990	6	1.860	8	99
$\pi/2$	10	11.628	12	1.506	8	27
$\pi/2$	20	11.907	12	1.723	10	49
$\pi/2$	30	11.959	12	1.807	11	73
$\pi/2$	40	11.977	12	1.850	11	97
$\pi/3$	10	19.338	20	1.518	12	27
$\pi/3$	20	19.836	20	1.729	13	50
$\pi/3$	30	19.927	20	1.806	13	78
$\pi/3$	40	19.959	20	1.846	13	110

TABLE 2

Fundamental eigenvalues of double right spherical triangles ($a = b = 0$) using variable grid ϕ-spacings ($\gamma = 2, \frac{1}{2}$)

Spherical triangle parameter Θ	*Rectangular grid parameters* $N_\theta = N_\phi$	*Fundamental eigenvalue* λ		
		Calculated value ($\gamma = 2$)	*Exact value*	*Calculated value* ($\gamma = \frac{1}{2}$)
π	10	5.750	6	5.118
π	20	5.931	6	5.592
π	30	5.969	6	5.773
π	40	5.983	6	5.856
$\pi/2$	10	11.368	12	10.692
$\pi/2$	20	11.798	12	11.739
$\pi/2$	30	11.910	12	11.919
$\pi/2$	40	11.949	12	11.969
$\pi/3$	10	19.123	20	19.061
$\pi/3$	20	19.609	20	19.888
$\pi/3$	30	19.825	20	19.961
$\pi/3$	40	19.902	20	19.979

and 0.002 for the $N_\theta = N_\phi = 20, 30, 40$ grids, respectively. The relative errors, for a given set of grid parameters, are smallest for $\Theta = \pi$ and largest for $\Theta = \pi/3$.

Table 2 shows the effects of variable grid ϕ-spacing. Grids in which the density of points increases symmetrically toward the poles ($\gamma = 2$) and, conversely, symmetrically toward the equator ($\gamma = \frac{1}{2}$), were considered with the same spherical triangles and grid parameters as previously. Variable grid spacing produces generally larger relative errors in the calculated λ except for the finer three grids when $\Theta = \pi/3$, in which case the results for λ when $\gamma = \frac{1}{2}$ are more accurate than the constant grid spacing results. When $\gamma = \frac{1}{2}$ and $\Theta = \pi/3$, the relative error in λ is approximately 0.047 for the $N_\theta = N_\phi = 10$ grid, but 0.006, 0.002, and 0.001 for the 20, 30, and 40 grids, respectively. Apparently, variable grid spacing to account for the singularity in ϕ can produce more accurate calculated values for λ, depending upon the particular characteristics of the spherical triangle.

Table 3 is limited to $\Theta = 2\pi$ only, in which the degenerate domain is the upper hemisphere with boundaries consisting of the equator and one meridional great circle arc (a "slit") between the north pole and equator and where λ was analytically found to be $\frac{15}{4}$. With constant grid spacing, the convergence in λ is monotonically decreasing, in contrast to previous results.

TABLE 3

Fundamental eigenvalue of slit upper hemisphere ($a = b = 0$; $\Theta = 2\pi$) using constant grid spacing ($\gamma = 1$)

Rectangular grid parameters $N_\theta = N_\phi$	*Fundamental eigenvalue* λ		*Optimal scalar relaxation factor* ω	*Required number of outer iterations* m	*Required number of S.O.R. inner iterations at convergence* k_m
	Calculated value	*Exact value*			
10	3.845	3.75	1.385	10	21
20	3.826	3.75	1.647	10	42
30	3.806	3.75	1.760	10	59
40	3.794	3.75	1.837	9	83

The degenerate case of the spherical wedge appears in Table 4. When $\Theta = \pi$ with $a = 0$, $b \to -\infty$, the wedge becomes a hemisphere, with $\lambda = 2$, as given by equation (34). When $\pi < \Theta \leq 2\pi$ with $a = 0$, $b \to -\infty$, the relevant domain remains the hemispherical wedge, with $\lambda = 2$, since the only value of ϕ in the domain for $a = 0$, $b \to -\infty$, and $\pi < \theta < 2\pi$ is $\phi = 0$, the north pole, by inequality (7). For the quarter-spherical wedge ($\Theta = \pi/2$) and the hemispherical wedge, the convergence in λ is monotonically increasing and quite rapid, with the refinement in grids. When $\Theta = 3\pi/2, 2\pi$, the convergence in λ is also monotonically increasing, but at a considerably reduced rate, probably because a larger proportion of the grid points are "superfluous," i.e., occur outside the spherical wedge domain.

Table 5 considers so-called oblique spherical triangles representing the general problem with unknown fundamental eigenvalue. A parametric family of spherical triangles $R(\Theta, 0,$

TABLE 4

Fundamental eigenvalues of spherical wedges ($a = 0, b \to -\infty$) using constant grid spacing ($\gamma = 1$)

Spherical triangle parameter Θ	*Rectangular grid parameters* $N_\theta = N_\phi$	*Fundamental eigenvalue* λ		*Optimal scalar relaxation factor* ω	*Required number of outer iterations* m	*Required number of S.O.R. inner iterations at convergence* k_m
		Calculated value	*Exact value*			
$\pi/2$	10	5.926	6	1.543	8	29
$\pi/2$	20	5.982	6	1.750	8	54
$\pi/2$	30	5.992	6	1.808	9	95
$\pi/2$	40	5.995	6	1.854	9	122
π	10	1.977	2	1.572	6	31
π	20	1.994	2	1.774	6	59
π	30	1.997	2	1.824	6	101
π	40	1.999	2	1.838	6	177
$3\pi/2$	10	1.828	2	1.512	6	26
$3\pi/2$	20	1.852	2	1.722	6	48
$3\pi/2$	30	1.917	2	1.830	6	73
$3\pi/2$	40	1.961	2	1.848	6	90
2π	10	1.929	2	1.465	6	23
2π	20	1.972	2	1.686	6	45
2π	30	1.982	2	1.788	6	62
2π	40	1.987	2	1.845	6	83

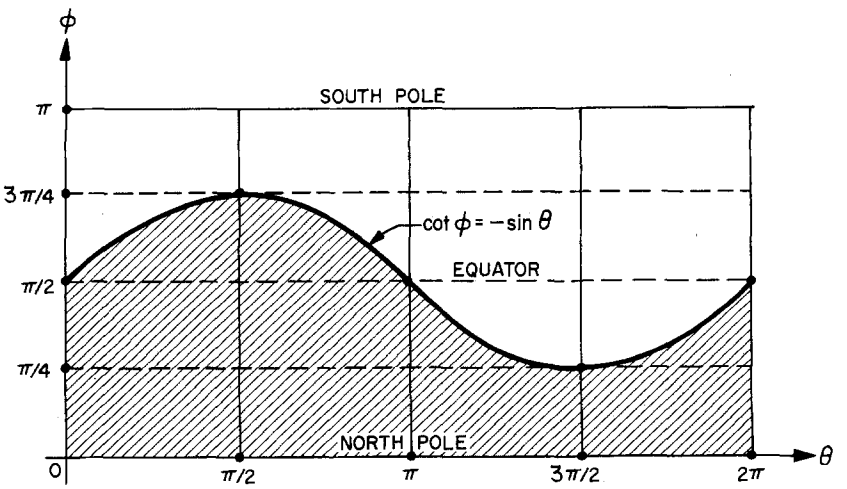

Figure 2. Interior domains of oblique spherical triangles defined by the parametric values $a = 0, b = -1; \Theta = \pi/2$, π, $3\pi/2$, and 2π (indicated by the shaded regions to the left of each of the four respective $\theta = \Theta$ values)

TABLE 5

Fundamental eigenvalues of oblique spherical triangles ($a = 0, b = -1$) *using constant grid spacing* ($\gamma = 1$)

Spherical triangle parameter Θ	*Rectangular grid parameters* $N_\theta = N_\phi$	*Calculated fundamental eigenvalue* λ	*Optimal scalar relaxation factor* ω	*Required number of outer iterations* m	*Required number of S.O.R. inner iterations at convergence* k_m
$\pi/2$	10	7.392	1.520	8	28
$\pi/2$	20	7.569	1.731	10	49
$\pi/2$	30	7.633	1.809	11	77
$\pi/2$	40	7.668	1.854	11	100
π	10	2.795	1.519	6	28
π	20	3.027	1.724	7	52
π	30	3.000	1.823	8	76
π	40	3.061	1.843	8	118
$3\pi/2$	10	2.435	1.476	8	24
$3\pi/2$	20	2.615	1.697	7	47
$3\pi/2$	30	2.631	1.796	8	66
$3\pi/2$	40	2.664	1.844	8	88
2π	10	2.396	1.435	8	22
2π	20	2.581	1.665	8	42
2π	30	2.597	1.771	8	57
2π	40	2.652	1.811	9	92

-1) is considered, where Θ assumes the values, $\pi/2$, π, $3\pi/2$, and 2π. The oblique plane $z = -y$ defines the non-meridional side (5c) of the spherical triangles and intersects the equator at an angle of $\pi/4$ at the points $\theta = 0$, π, and 2π (see Figure 2). For three Θ values, convergence of λ is monotonically increasing with the grid refinement, but when $\Theta = \pi$, oscillatory behavior in λ occurs, an anomaly which has previously been observed [13, pp. 351–352] in the numerical calculation of fundamental eigenvalues. Furthermore, when $\Theta = 3\pi/2$, 2π, the convergence in λ is less uniform than in the earlier results for known solutions, possibly as a consequence of the boundary transcendental curve in the θ, ϕ-plane (see Figure 2). The grid point approximation to the curved southern boundary of the oblique spherical triangle (present in the general problem) varies somewhat with the grid parameters N_θ, N_ϕ, a situation which was avoided in the earlier results when all boundaries coincided with constant-value θ and ϕ great circle arcs.

6. Problem of a spherical surface with a slit

6.1. *Boundary conditions for the slit domain*

The problem of determining the fundamental eigenvalue for a domain which is the exterior of a spherical "triangle" when $\Theta = 0$ will now be considered. In the limit, the triangle degenerates to a meridional great circle arc or "slit," which may be assumed, without loss of

generality, to extend from the spherical north pole along a great circle arc. The slit domain may be specified by a slit extension parameter Φ, where $0 < \Phi < \pi$, and is determined from equation (6) to be $\Phi = \operatorname{arccot} a = \arcsin(a^2 + 1)^{-\frac{1}{2}}$, with b arbitrary.

A rectangular uniform network of grid points (θ_i, ϕ_j), $i = 0, 1, \ldots, N_\theta$; $j = 0, 1, \ldots, N_\phi$ is superposed over the entire spherical surface, $0 \leq \phi \leq \pi$; $0 \leq \theta \leq 2\pi$, so that the relations between the number of grid intervals and the constant grid spacings are $h_\theta N_\theta = 2\pi$, and $h_\phi N_\phi = \pi$. In the θ, ϕ-plane, the slit appears along portions of three of the rectangular boundaries, viz., the entire line representing the north pole $\phi = 0$, and like portions of the two lines representing the slit meridian, $\theta = 0, 2\pi$. In general, the slit boundary will not terminate on a grid point.

The boundary conditions (8b) to be imposed on the discretized version of the eigenvalue equation for the spherical surface with a slit are $U_{i,0} = 0$ for all i at the north pole of the sphere, and $U_{0,j} = U_{N_\theta,j} = 0$, for all j such that $\phi_j \leq \Phi$, along the slit boundary. In general, non-zero $U_{i,j}$ occur on the rectangular grid boundary along the slit meridians beyond the extension of the slit ($U_{0,j}$ and $U_{N_\theta,j}$ for which $\phi_j > \Phi$) and at the south pole (U_{i,N_ϕ} for all i). The finite difference equation (17) is valid for all grid interior points (θ_i, ϕ_j), $i = 1, 2, \ldots, N_\theta - 1$; $j = 1, 2, \ldots, N_\phi - 1$, but must be modified for grid boundary points which do not coincide with the slit. Since the lines $i = 0, N_\theta$ coincide on the spherical surface, the following periodic boundary conditions must be imposed: $U_{0,j} = U_{N_\theta,j}$ for all j such that $\phi_j > \Phi$. Equation (17) may thus be extended to the line $i = N_\theta$ by replacing the undefined $U_{N_\theta+1,j}$ by $U_{1,j}$, for all j, as necessary, viz.,

$$a_j U_{N_\theta,j} - b_j U_{1,j} - c_j U_{N_\theta,j+1} - b_j U_{N_\theta-1,j} - c_{j-1} U_{N_\theta,j-1} = \lambda e_j U_{N_\theta,j} \quad \text{for } j = 1, 2, \ldots, N_\phi - 1, \text{ if } \phi_j > \Phi, \tag{37}$$

with a_j, b_j, c_j, and e_j defined as previously.

Difference equations for grid points at the south pole may be derived by integrating the partial differential equation (8a) over the disc $0 < \theta < 2\pi$; $\phi_{N_\phi - \frac{1}{2}} < \phi < \phi_{N_\phi} = \pi$ (see Figure 3). Because of the 2π periodicity in θ, it is seen that

$$-\int_{\theta=0}^{2\pi} u_\phi(\theta, \phi_{N_\phi - \frac{1}{2}}) \sin \phi_{N_\phi - \frac{1}{2}} d\theta + \lambda \int_{\theta=0}^{2\pi} \int_{\phi_{N_\phi - \frac{1}{2}}}^{\pi} u \sin \phi \, d\phi \, d\theta = 0. \tag{38}$$

The first integral may be approximated, by the centered first difference quotient (14), as the finite sum,

$$-\sum_{i=1}^{N_\theta} \left(\frac{U_{i,N_\phi} - U_{i,N_\phi - 1}}{h_{\phi,N_\phi}} \right) h_\theta \sin \phi_{N_\phi - \frac{1}{2}}, \tag{39}$$

while the second term may be approximated by

$$\lambda U_{i,N_\phi}(2\pi)[-\cos \phi]\Big|_{\phi_{N_\phi - \frac{1}{2}}}^{\pi} = 2\pi\lambda U_{i,N_\phi}(1 + \cos \phi_{N_\phi - \frac{1}{2}}). \tag{40}$$

Of course, U_{i,N_ϕ} represents the unique approximate value (which may arbitrarily be denoted U_{1,N_ϕ}) of the solution u at the south pole for all i. Substituting these approximations in

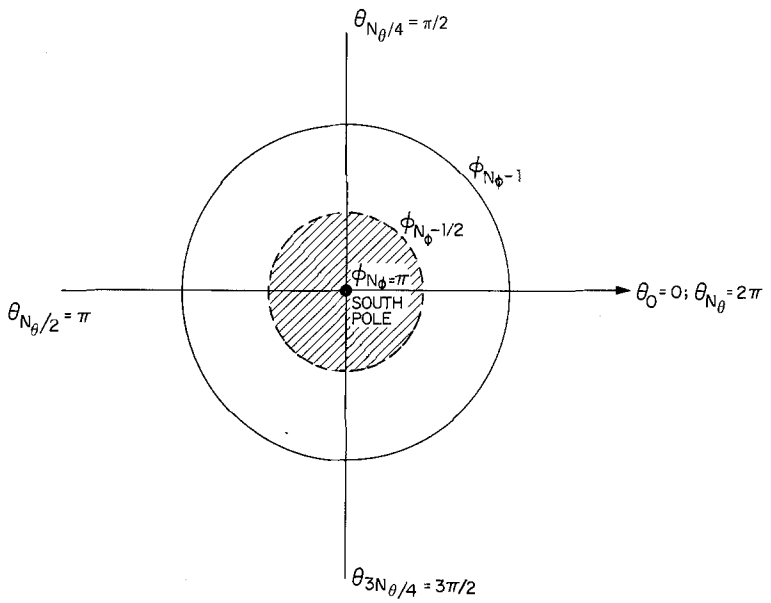

Figure 3. Disc (indicated by shading) utilized to derive difference equations valid at the spherical south pole.

equation (38) and re-arranging yields

$$\frac{2 \sin \phi_{N_\phi - \frac{1}{2}}}{h_{\phi, N_\phi}} \sum_{i=1}^{N_\theta} (U_{i, N_\phi} - U_{i, N_\phi - 1}) = \frac{4\pi}{h_\theta} (1 + \cos \phi_{N_\phi - \frac{1}{2}}) \lambda U_{i, N_\phi}. \tag{41}$$

Define

$$e_{N_\phi} = \frac{4\pi}{h_\theta} (1 + \cos \phi_{N_\phi - \frac{1}{2}}), \tag{42}$$

which, by equation (12), may be rewritten as

$$e_{N_\phi} = 2N_\theta (1 - \sin \tfrac{1}{2} \phi_{N_\phi - 1}) > 0. \tag{43}$$

Equation (41) may thus be written, using definitions (18b) and (42), as a finite $(N_\theta + 1)$-point difference equation for the component of U at the south pole:

$$c_{N_\phi - 1} (N_\theta U_{1, N_\phi} - \sum_{i=1}^{N_\theta} U_{i, N_\phi - 1}) = \lambda e_{N_\phi} U_{1, N_\phi}. \tag{44}$$

6.2. *Solution for the fundamental eigenvalue*

The finite difference equations may again be written in matrix form as $AU = \lambda EU$, where the power method and the S.O.R. iterates are used to approximate λ. The vector dimensionality of U is equal to the number of grid interior points, $(N_\theta - 1)(N_\phi - 1)$, plus

the number of grid boundary points along the slit meridian beyond the slit, including the single south polar point. The point S.O.R. method utilizes equation (26) for grid interior points; for grid boundary points along the slit $i = N_\theta$, in accordance with equation (37),

$$U_{N_\theta,j}^{(k+1)} = \frac{\omega}{a_j}[b_j U_{1,j}^{(k+1)} + c_j U_{N_\theta,j+1}^{(k)} + b_j U_{N_\theta-1,j}^{(k+1)} + c_{j-1} U_{N_\theta,j-1}^{(k+1)} + F_{N_\theta,j}] + (1-\omega)U_{N_\theta,j}^{(k)}$$
$$\text{for } j = 1, 2, \ldots, N_\phi - 1, \text{ if } \phi_j > \Phi;\ k = 1, 2, \ldots \qquad (45)$$

The iterates associated with the south pole, are, in accordance with equation (44),

$$U_{1,N_\phi}^{(k+1)} = \frac{\omega}{N_\theta}\left[\sum_{i=1}^{N_\theta} U_{i,N_\phi-1}^{(k+1)} + \frac{F_{1,N_\phi}}{c_{N_\phi-1}}\right] + (1-\omega)U_{1,N_\phi}^{(k)}, \qquad k = 1, 2, \ldots \qquad (46)$$

Due to the complicated nature of the difference equation (44) at the south pole, the Jacobi matrix associated with A is not necessarily cyclic of index 2, as previously. Thus, the expression (30) for ω_{opt} no longer rigorously applies, and the actual optimal ω is unknown. However, it has been suggested [13, p. 262] that the value produced by the formula (30) may be reasonably close to the unknown optimal ω, even under such conditions. For this reason, the expression (30) is used for approximating ω_{opt} in the computer algorithm, described in detail in [15], used to produce the numerical results that follow.

6.3. *Numerical results*

Table 6 displays calculated values of λ for each $\Phi = n(\pi/8)$, $n = 1, 2, \ldots, 7$ and for the usual rectangular grids, assuming uniform grid spacing ($\gamma = 1$) throughout. The convergence in λ with increasing grid refinement for given Φ is by no means monotonic, in contrast to most of the spherical triangle problem results. Note that convergence in λ occurs more slowly (1) for a finer grid than for a coarse grid, and (2) as the slit extent decreases. The generally slower convergence of the S.O.R. iterations, in comparison with the problem of the spherical triangle, is related to the fact that the optimal ω is unknown for the slit problem.

Further investigations were conducted for values of Φ near the polar limits $0, \pi$ for the slit boundary (Table 7). To avoid singularities at the poles, two values, Φ_1 and Φ_2, such that $0 < \Phi_1 < \pi/N_\phi$ and $\pi - (\pi/N_\phi) < \Phi_2 < \pi$ were assumed by Φ so that none of the grid points, except those at the north pole, would coincide with the slit boundary (for $\Phi_1 \cong 0$) and so that all of the grid points along the slit meridian, except those at the south pole, would coincide with the slit boundary (for $\Phi_2 \cong \pi$), regardless of N_ϕ. The calculated λ display a monotonic decrease for $\Phi \cong 0$ and a monotonic increase for $\Phi \cong \pi$, with the grid refinement, and are in agreement with the Table 6 trend. The calculated λ as a function of Φ are graphed for three grids in Figure 4 ($N_\theta = N_\phi = 30$ is omitted to preserve legibility). A nearly linear relationship is observed, with a slope, $d\lambda/d\Phi \cong 0.2$ (radians)$^{-1}$. The case $\Phi = \pi$ was previously solved analytically, as the limit of a spherical wedge domain, for the exact value $\lambda = \frac{3}{4}$, a result in excellent agreement with Table 7 and Figure 4. The limit as $\Phi \to 0$ (and the slit spherical surface degenerates to a punctured sphere) tends rather slowly, in Figure 4 and Table 7, to the true value $\lambda = 0$, with the grid refinement. The use of still finer grids in which $N_\phi > 40$ indicates (Table 8) that this convergence, $\lambda \to 0$, proceeds quite gradually.

TABLE 6

Fundamental eigenvalues of a spherical surface with a slit

Slit extension parameter Φ	*Rectangular grid parameters* $N_\theta = N_\phi$	*Calculated fundamental eigenvalue* λ	*Near-optimal scalar relaxation factor* ω	*Required number of outer iterations* m	*Required number of S.O.R. inner iterations at convergence* k_m
$\pi/8$	10	0.209	1.794	4	90
$\pi/8$	20	0.193	1.900	4	195
$\pi/8$	30	0.188	1.937	5	283
$\pi/8$	40	0.199	1.960	5	317
$\pi/4$	10	0.263	1.773	4	80
$\pi/4$	20	0.273	1.883	5	164
$\pi/4$	30	0.259	1.926	5	245
$\pi/4$	40	0.265	1.953	5	271
$3\pi/8$	10	0.317	1.755	5	73
$3\pi/8$	20	0.325	1.874	5	150
$3\pi/8$	30	0.327	1.917	5	223
$3\pi/8$	40	0.329	1.949	5	242
$\pi/2$	10	0.427	1.722	5	61
$\pi/2$	20	0.406	1.860	5	133
$\pi/2$	30	0.399	1.910	5	198
$\pi/2$	40	0.396	1.941	5	229
$5\pi/8$	10	0.486	1.705	5	56
$5\pi/8$	20	0.465	1.851	5	122
$5\pi/8$	30	0.457	1.905	5	180
$5\pi/8$	40	0.469	1.936	5	203
$3\pi/4$	10	0.550	1.688	5	51
$3\pi/4$	20	0.563	1.835	5	104
$3\pi/4$	30	0.544	1.884	5	182
$3\pi/4$	40	0.551	1.897	6	295
$7\pi/8$	10	0.619	1.668	6	46
$7\pi/8$	20	0.637	1.811	6	100
$7\pi/8$	30	0.644	1.860	6	169
$7\pi/8$	40	0.647	1.880	6	262

7. Singularities in three-dimensional problems

Let $v(x, y, z)$ be the solution of the Dirichlet problem (1) in a polyhedral domain G. The singular behavior of v in a neighborhood of a vertex of G is of interest. Knowledge about this problem is quite limited [4, 5], as mentioned earlier; however, an intuitive idea of what to expect may be obtained from the following considerations. Assume a vertex of G is placed at the origin O, and, as before, let D be the intersection of the domain G and the surface of a small sphere with center at O. If $u(\theta, \phi)$ is a solution of the eigenvalue problem (4), and if σ is

TABLE 7

Fundamental eigenvalues of a spherical surface with a slit near slit boundary polar limiting values

Slit extension parameter Φ	*Rectangular grid parameters* $N_\theta = N_\phi$	*Calculated fundamental eigenvalue* λ	*Near-optimal scalar relaxation factor* ω	*Required number of outer iterations* m	*Required number of S.O.R. inner iterations at convergence* k_m
0	10	0.147	1.825	4	110
0	20	0.123	1.919	4	249
0	30	0.112	1.950	4	383
0	40	0.105	1.971	4	459
π	10	0.697	1.646	6	40
π	20	0.724	1.790	6	87
π	30	0.733	1.843	6	143
π	40	0.737	1.863	6	222

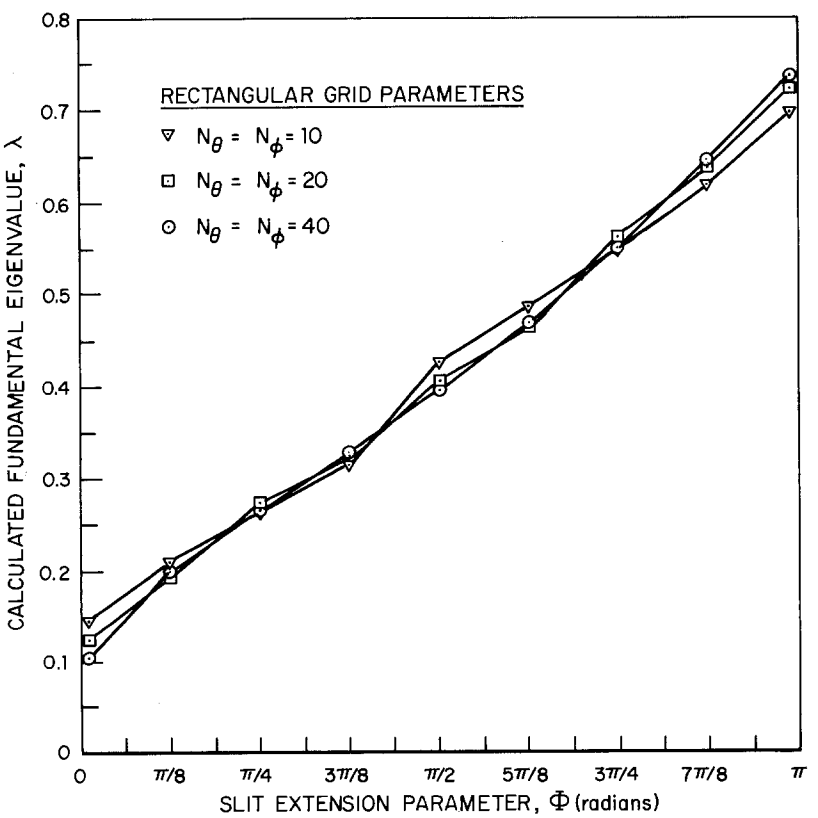

Figure 4. The calculated fundamental eigenvalue λ as a function of the slit extension parameter Φ for various rectangular grids (N_θ by N_ϕ intervals).

TABLE 8

Fundamental eigenvalue of a punctured spherical surface ($\Phi \to 0$)

Rectangular grid parameter, N_ϕ	*Calculated fundamental eigenvalue,* λ
50	0.1005
60	0.0969
70	0.0942
80	0.0919
90	0.0899
100	0.0883
120	0.0856
140	0.0834
160	0.0816
180	0.0800
200	0.0787

defined by $\sigma^2 + \sigma = \lambda$, then the function $w = r^\sigma u(\theta, \phi)$ is a harmonic function which vanishes on the sides of G that are near O. In order that w have square-integrable first derivatives, choose σ to be the larger root of the quadratic, viz., $\sigma = (\sqrt{1 + 4\lambda} - 1)/2$. If λ is the fundamental eigenvalue of problem (4), then the smallest possible value of σ results, and hence the worst singularity in w. Since $w \approx r^\sigma$ as $r \to 0$, it is reasonable to expect also that $v \approx r^\sigma$ as $r \to 0$, with corresponding asymptotic behavior for the derivatives of v.

The domain G has two kinds of singularities near the vertex O. The surface ∂G is not smooth at each of the edges of the polyhedron which emanate from the origin, and this geometry produces "edge singularities." The conjectured behavior $v \approx r^\sigma$ may be thought of as representing another type of singularity, the "vertex singularity" of v. The edge

TABLE 9

Vertex singularities for some degenerate polyhedra

Slit extension parameter Φ	*Calculated* fundamental eigenvalue* λ	*Corresponding vertex singularity* σ
0	0	0
$\pi/8$	0.199	0.170
$\pi/4$	0.265	0.218
$3\pi/8$	0.329	0.261
$\pi/2$	0.396	0.304
$5\pi/8$	0.469	0.348
$3\pi/4$	0.551	0.395
$7\pi/8$	0.647	0.447
π	0.75	0.5

* Theoretical values for λ and σ are given for the limits, $\Phi = 0, \pi$.

singularities are present in the eigenfunctions u of problem (4). The edges of G that emanate from O correspond to vertices in the spherical polygon D. If D has an angle α, then the corresponding edge singularity in u is $\rho^{\pi/\alpha}$, where $\rho(x, y, z)$ is the distance from a point (x, y, z) of G to the edge of G passing through the vertex of D with angle α [1]. As $\alpha \to 2\pi$, the corresponding edge singularity approaches $\rho^{\frac{1}{2}}$, which is the worst possible case.

The vertex singularity σ depends on the geometry of G near the vertex. Table 9 presents values of σ which correspond to the λ given in Table 6 for the finest grids ($N_\theta = N_\phi = 40$). The domain G, in this case, is a degenerate "slit polyhedron" which may be described as follows. If O is any point in the interior of a given polyhedron, then G consists of all the points of the polyhedron except those which lie on a plane sector with angle Φ and apex situated at O. The point O is considered to be a vertex of the "slit polyhedron." In a similar manner, the methods of this paper may be used to calculate the value of σ for each vertex of any polyhedron G by solving the corresponding eigenvalue problem.

REFERENCES

[1] Neil M. Wigley, Asymptotic expansions at a corner of solutions of mixed boundary value problems, *Journal of Mathematics and Mechanics*, Vol. 13, No. 4, pp. 549–576, July 1964.

[2] V. A. Kondrat'ev, Boundary problems for elliptic equations in domains with conical or angular points, *Transactions of the Moscow Mathematical Society*, Vol. 16, pp. 209–292, 1967; translated and published by the American Mathematical Society, 1968.

[3] George C. Sih, editor, *Methods of analysis and solutions of crack problems*, Leyden: Noordhoff International Publishing, 1973.

[4] R. B. Kellogg, Singularities in interface problems, pp. 351–400 in *Numerical Solution of Partial Differential Equations - II*, edited by Bert Hubbard, New York and London: Academic Press, 1971.

[5] Pierre Grisvard, Behavior of the solutions of an elliptic boundary value problem in a polygonal or polyhedral domain, pp. 207–274 in *Numerical Solution of Partial Differential Equations - III*, edited by Bert Hubbard, New York and London: Academic Press, 1976.

[6] Zdeněk P. Bažant, Three-dimensional harmonic functions near termination or intersection of gradient singularity lines: A general numerical method, *International Journal of Engineering Science*, Vol. 12, No. 3, pp. 221–243, March 1974.

[7] Zdeněk P. Bažant and Leon M. Keer, Singularities of elastic stresses and of harmonic functions at conical notches or inclusions, *International Journal of Solids and Structures*, Vol. 10, No. 9, pp. 957–964, September 1974.

[8] J. A. Morrison and J. A. Lewis, Charge singularity at the corner of a flat plate, *SIAM Journal on Applied Mathematics*, Vol. 31, No. 2, pp. 233–250, September 1976.

[9] R. Courant and D. Hilbert, *Methods of Mathematical Physics*, Volume I, New York: Interscience Publishers, 1953.

[10] Brice Carnahan, H. A. Luther and James O. Wilkes, *Applied Numerical Methods*, New York and London: John Wiley & Sons, 1969.

[11] Richard S. Varga, *Matrix Iterative Analysis*, Englewood Cliffs, N.J.: Prentice-Hall, 1962.

[12] Eugene Isaacson and Herbert B. Keller, *Analysis of Numerical Methods*, New York and London: John Wiley & Sons, 1966.

[13] George E. Forsythe and Wolfgang R. Wasow, *Finite-Difference Methods for Partial Differential Equations*, New York and London: John Wiley & Sons, 1960.

[14] James M. Ortega, *Numerical Analysis: A Second Course*, New York and London: Academic Press, 1972.

[15] Harvey Walden, Solution of an eigenvalue problem for the Laplace operator on a spherical surface, Document No. X-582-74-41, NASA/Goddard Space Flight Center, February 1974.